

Benchmarking Deep Learning Classifiers: Beyond Accuracy

Wei Dai, Daniel Berleant

Abstract— Previous research evaluating deep learning (DL) classifiers has often used top-1/top-5 accuracy. However, the accuracy of DL classifiers is unstable in that it often changes significantly when retested on imperfect or adversarial images. This paper adds to the small but fundamental body of work on benchmarking the robustness of DL classifiers on imperfect images by proposing a two-dimensional metric, consisting of mean accuracy and coefficient of variation, to measure the robustness of DL classifiers. Spearman’s rank correlation coefficient and Pearson’s correlation coefficient are used and their independence evaluated. A statistical plot we call mCV is presented which aims to help visualize the robustness of the performance of DL classifiers across varying amounts of imperfection in tested images. Finally, we demonstrate that defective images corrupted by two-factor corruption could be used to improve the robustness of DL classifiers. All source codes and related image sets are shared on a website (<http://www.animpala.com>) to support future research projects.

Index Terms—benchmark metrics, defective images, robust deep learning, machine learning

1 INTRODUCTION

Computer scientists and engineers have innovated many benchmark tools to measure hardware devices and compare software algorithms. Well-known, non-profit benchmark organizations include Standard Performance Evaluation Corporation (SPEC) [1], Transaction Processing Performance Council (TPC) [2], Storage Performance Council (SPC) [3], and Machine Learning Performance (MLPerf) [4]. These evaluate CPUs, databases, storage, and machine learning respectively. MLPerf has measured the training and inference performance of ML hardware, software, and services. All these organizations aperiodically update their benchmark tools, retire obsolete benchmark programs, and officially publish on their websites.

Deep learning (DL) classifiers have been shown to work well on high quality image sets. DL classifiers have classified objects in high quality image sets, for example, at 97.3% accuracy, which is better than human capabilities [5]. However, low quality sets present a more challenging environment. If the data is imperfect, as real data so often are, how will results be affected? In [6], the researchers discovered that human visual systems are more robust than DL classifiers when images are manipulated by contrast reduction, additive noise, and eidolon distortions. In [7], DL classifier performance was lower than that of humans when recognizing images corrupted with Gaussian noise or Gaussian blur.

DL classifiers can also make mistakes on even high quality images in the DL security field. For example, an adversarial image may be a high quality image modi-

fied by tiny corruptions chosen to confuse DL classifiers. Even though humans may not notice these corruptions, these deliberately modified images can confuse DL classifiers, reducing their accuracy [8], [9], [10]. Therefore, the robustness of DL classifiers across image corruption conditions will continue to merit attention. To measure robustness of DL classifiers, we can expect a robust DL classifier to have both high accuracy as well as low variance across the corruption conditions.

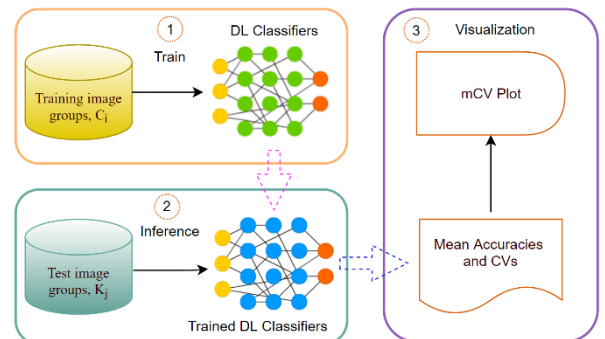


Figure 1. An architecture of benchmarking DL classifiers. There are three stages when measuring the robustness of DL classifiers. Step 1 trains DL classifiers. Step 2 performs inference using the trained DL classifiers. Step 3 depicts the average accuracies and coefficient of variation (CV for short) through the mCV plot.

In this paper, our contributions are as follows:

- 1) We proposed a two-dimensional metric, including mean accuracy and coefficient of variation to benchmark the robustness of DL classifiers. The new metric is not bound to any specific DL classifiers. Spearman’s Rank correlation coefficient and Pearson correlation coefficient are used for analyzing the two putatively independent variables.

• Dr. Wei Dai is with the Department of Computer Science, Southeast Missouri State University, Cape Girardeau, MO 63701. E-mail: wdai@semo.edu.

• Dr. Daniel Berleant. is with the Department of Information Science, University of Arkansas at Little Rock, Little Rock, AR 72204. E-mail: dberleant@ualr.edu.

2) We developed a new statistical visualization named the mCV plot for comparing the robustnesses of DL classifiers.

3) Test image sets had 69 test image groups, consisting of one clean image and 68 defective images. We created 68 test image sets which were each corrupted by two different corruptions. Compared with clean images, training with two-factor corrupted image sets can improve the robustness of DL classifiers. These image sets and source codes are shared on a website (<http://www.animpala.com/>) to support additional research projects.

4) We implemented some tests using the two-dimensional metric and show the resulting mCV plots in Figs. 2-6.

The rest of this paper is structured as follows. Section 2 discusses related work. In Section 3, we provide the research design and methodology. Section 4 introduce the experimental results. Discussion and Conclusion constitute Section 5 and Section 6, respectively.

2 RELATED WORK

Researchers have discovered that DL classifiers are fragile when faced with image corruptions. In [11], the authors demonstrated that the Google Cloud Vision API could be misled after adding approximately 14.25% impulse noise density. In [12], DL classifiers had reduced accuracy of classification when testing five types of quality distortions, including JPEG/JPEG2000 compression, blur, Gaussian noise, and contrast. There have been various previously reported corruptions imposed on high quality ImageNet datasets. In [13] the authors created 15 types of single corruption, including noise, blur, and brightness. In [14][7], the authors used Gaussian noise or Gaussian blur to change images. Previous research projects created defective images via single factor corruptions. However, 69 benchmarking image sets, including a clean set, sets with single factor corruptions, and sets with two-factor corruption conditions, for benchmarking image sets were discussed in [15]. That study demonstrated that training DL classifiers on two-factor corrupted image sets could improve their robustness.

Previous researchers have measured the robustness of DL classifiers via top-1 or top-5 precision analyses [16]. For example [13] chose the average rates of correct ("Top-1") and almost correct ("Top-5") classifications, the authors setting the Top-1 error rate of AlexNet as the reference error rate. In contrast, we provided a two-dimensional metric, consisting of mean accuracy and CV. This supports characterizing the stability of DL classifiers as having high mean accuracy along with small coefficient variance of accuracies across corruption conditions.

Note that the coefficient of variation defines the ratio of the standard deviation to the mean. The coefficient of variation is used in different fields, including physics, medicine, chemistry, and engineering [17], [18]. In agriculture, Francis and Kannenberg [19] used the mean yield and coefficient of variation to analyzing

yield stability. The CV offers a way to help differentiate the variation from the mean because, compared to using variance, CV is less affected by mean. A CV of 2% indicates less variation for a given mean than a CV of, say, 15%. So, when judging a DL classifier, we can measure the average accuracy, \bar{x} , and the coefficient of variation, CV, as they say different things. A high accuracy and small CV for a DL classifier is better than a low accuracy with a large CV.

Spearman's rank correlation coefficient is a statistic used for calculating the strength of a monotonic relationship between paired data, (X,Y), in a sample N. Assume that a value of X has rank K and its corresponding value of Y has rank L. As shown in Eq. 1, Spearman's rank (r_{xy}) can be calculated for the sample data N.

$$r_{xy} = 1 - \frac{6 \sum d_{xy}^2}{n(n^2 - 1)} \quad \text{Eq. 1}$$

where d_i is the difference between K and L, and $d_{xy}^2 = (K - L)^2$. The number of data in N is n.

The Pearson correlation coefficient is used for evaluating the strength of a linear relationship between two random variables. The Pearson correlation coefficient, r_{xy} , can be calculated as in Eq. 2.

$$r_{xy} = \frac{\sum_i^n (x_i - \bar{x})(y_i - \bar{y})}{\sqrt{\sum_i^n (x_i - \bar{x})^2} \sqrt{\sum_i^n (y_i - \bar{y})^2}} \quad \text{Eq. 2}$$

where x_i, y_i are paired datasets indexed with i. \bar{x}, \bar{y} are means. The sample size is n.

Previous researchers has usually offered tables, line diagrams, and bar charts to display accuracy of DL classifiers. We supplement those tools with a new statistical graphic, the mCV plot, that integrates two metrics (mean accuracy and CV), and includes four groups and a reference point.

3 RESEARCH DESIGN AND METHODOLOGY

For evaluating the robustnesses of DL classifiers, we start with the fundamental assumption that a one DL classifier is more robust than another if it has higher accuracy and smaller coefficient of variation. The coefficient of variation is derived from the standard deviation (σ), which is a measure of spread of distributions in statistics. A larger σ denotes that the population of the sample data is further dispersed from the mean. A smaller σ indicates the population of sample data is more clumped together.

In statistics, the formula for standard deviation (σ) is shown in Eq. 3.

$$\sigma = \sqrt{\frac{\sum_{i=1}^n (x_i - \mu)^2}{n}} \quad \text{Eq. 3}$$

where x_i , n, and μ are a data value, the number of data, and the mean, respectively.

When testing performance across a group of data

sets, we can collect the mean of the accuracies, μ , and the standard deviation of the accuracies, σ . We should compare the σ of two or more DL classifiers when their μ are the same or similar, because if two DL classifiers have the same mean accuracies, a small variation (σ) for a DL classifier shows better stability in its performance across image quality conditions than a large variation. We can say that a smaller variation (σ) indicates that the DL classifier is more dependable. In brief, we want a DL classifier to have a high accuracy with small standard deviation.

The coefficient of variation (or CV) denotes the standard deviation as a percentage of the mean as shown in Eq. 4.

$$CV \% = 100 \times \frac{\sigma}{\mu} \quad \text{Eq. 4}$$

where σ is the population standard deviation, and the mean, μ , is the average of the data sets.

Suppose that we wish to compare performances of DL classifiers. We propose a four-quadrant statistical plot approach which we name mCV (for **m**ean accuracy and **c**oefficient of **v**ariation) plot. In this statistical plot, the Y-axis and X-axis indicate mean accuracy and coefficient of variation, respectively. Then, the mean accuracy and CV of a reference point splits the figure into four groups as shown in Figure 2.

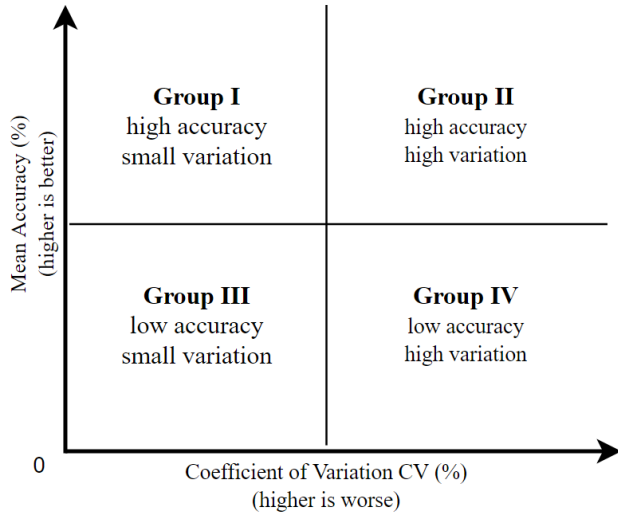


Figure 2. mCV plot. The Y-axis and X-axis indicate mean accuracy and coefficient of variation, respectively. The mean accuracy and CV of a reference point divided the above plot into four groups: Group I, Group II, Group III, and Group IV.

In Figure 2, clockwise from top left, are Group I, Group II, Group III, and Group IV, respectively. The Group I has high accuracy and low variation; the Group II has high accuracy and high variation; the Group III has low accuracy and low variation; and the Group IV has low accuracy and high variation.

The algorithm of how to split DL classifiers into four groups is shown in Algorithm 1.

Algorithm 1: Place a DL classifier into a group (quadrant) of the mCV graph.

```

Input: DL mean accuracy  $m$ , DL CV  $v$ 
Output: group number
IdentifyGroup (DL meanAccuracy  $m$ , DL CV  $v$ )
{
     $m_r \leftarrow$  reference accuracy
     $v_r \leftarrow$  reference CV
    if ( $m \geq m_r$  and  $v \leq v_r$ ) return "Group I"
    if ( $m \geq m_r$  and  $v > v_r$ ) return "Group II"
    if ( $m < m_r$  and  $v \leq v_r$ ) return "Group III"
    if ( $m < m_r$  and  $v > v_r$ ) return "Group IV"
}

```

A trained DL classifier is notated as $\mathbf{D}_{trainsets}^{testsets}$, where \mathbf{D} refers to the DL classifier's name, testsets refers to a group of test sets, and trainsets refers to a group of training sets. Then, we test the accuracy rate on every corruption type, c . Different c values are different corruption types, and level of severity is s , with $s \in \{0.1, 0.15, 0.2\}$ when doing SP or GA corruptions, and a $s \in \{-60^\circ, -30^\circ, 0^\circ, 30^\circ, 60^\circ\}$ when doing rotation corruptions. The accuracy rate is written $Accu(\mathbf{D})$ as shown in Eq. 5.

$$Accu(\mathbf{D}) \% = 100 \times \frac{\sum_{k=1}^n Accu(\mathbf{D}_{trainset_c}^{testset_k})}{n}, \quad \text{Eq. 5}$$

where both c and k mean a corruption type, respectively. Each possible value of c and k , from type-1 to type-69, is specified in Table 3.

For example, we can define $AlexNet_{clean}^{alltests}$ to denote the AlexNet classifier trained on a clean image set, and tested on all 69 different test image sets. $AlexNet_{SP0.1RL30}^{alltests}$ will denote the AlexNet classifier trained on an image set corrupted by SP0.1 then corrupted more by RL30 (rotate left 30°), and the classifier is tested on all 69 test image sets.

$$CV(\mathbf{D}) \% = 100 \times \frac{\sigma}{\mu} \quad \text{Eq. 6}$$

$$= 100 \times \sqrt{\frac{\sum_{k=1}^{69} (Accu(\mathbf{D})_k - \overline{Accu(\mathbf{D})})^2}{n}}$$

where $CV(\mathbf{D})$ indicates the coefficient of variation of mean accuracies of a DL classifier. $\overline{Accu(\mathbf{D})}$ denotes the mean accuracies of the DL classifier. $Accu(\mathbf{D})$ means the accuracy of the DL classifier. Variable k , $k \in [1, 69]$, is the testing image group (For more information, see attached Table 3).

The training data sets consist of nine training sets: a clean image set and eight corrupted image sets. Each training group has 500 images. The clean image set contains the original images. The eight corrupted im-

age sets are corrupted by SP0.1, GA0.1, SP0.1GA0.1, GA0.1SP0.1, SP0.1RL30, SP0.1RR30, RL30, and RR30.

Each testing set contains one clean image group and 68 corrupted image groups. The clean image group contained original images. Each testing group has 500 images. The training sets and testing sets have no overlap. In other words, if a image exists in a training group, the image will not be found in any testing groups.

4 EXPERIMENTAL RESULTS

4.1 Benchmarking Three DL classifiers on clean images

In this experiment, the average of the CVs of the AlexNet, ResNet50, and VGG19 classifiers and the average of their mean accuracies defined the reference point.

Because abbreviated notations might not be easily read in Figure 3, we wrote labels instead. For example, the label “AlexNet(clean)” denotes the AlexNet network trained on the unmodified CIFAR-10 image set. In Table 1, the training data sets of CIFAR-10 are different for each row, but the testing was on all 69 data sets including the clean CIFAR-10 image set and 68 corrupted versions, which we may denote as $\text{AlexNet}_{\text{clean}}^{\text{alltests}}$.

As shown in Figure 3 below, the mean accuracy of the ResNet50 classifier is better than AlexNet, but the CV of the ResNet-50 is higher (thus worse) than for AlexNet. The VGG19 has the worst CV and the best mean accuracy of those DL classifiers. Thus the mCV plot visualizes a comparison of different DL classifiers on the same test protocol.

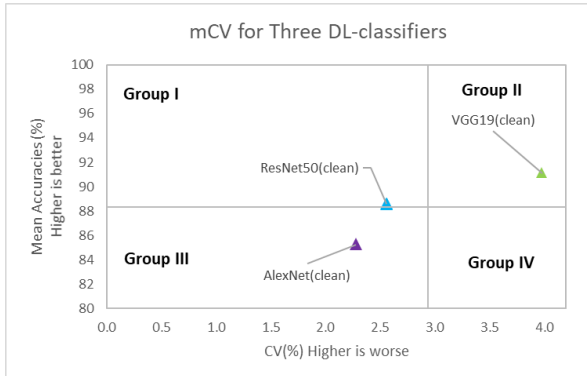


Figure 3. The mCV plot for three DL classifiers on the CIFAR-10 dataset and tested on all 69 test sets. The reference value, $(\text{CV, Accuracy})=(2.94\%, 88.31\%)$, is the average of ResNet(clean), AlexNet(clean), and VGG(clean).

4.2 Benchmarking the AlexNet classifier on corrupted images

As shown in Figure 4, the red triangle labeled “AlexNet(clean)” represents the AlexNet classifier trained on clean data. The purple points represent the AlexNet classifiers trained on corrupted image sets. From Figure 4, we can see the following.

1. The training datasets affected prediction CVs of the

AlexNet classifiers. Notably, after training AlexNet on corrupted images, the CVs are less than when training is limited to clean images.

2. Training AlexNet on corrupted images can improve the mean accuracy during testing. Specifically, most $\text{Accu}(\text{AlexNet}_{\text{alltests}}^{\text{corrupt}})$ values are higher than $\text{Accu}(\text{AlexNet}_{\text{clean}}^{\text{alltests}})$. That is, tested accuracies tend to be better when training sets contain images that have been corrupted by degradation with common forms of noise and distortion.

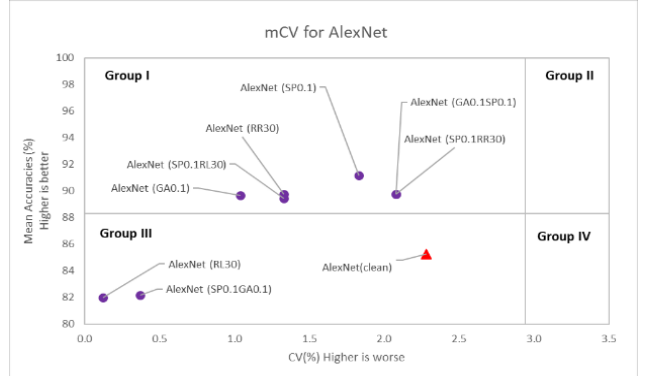


Figure 4. The mCV plot for AlexNet after corrupted image groups were used to train the DL classifier on the CIFAR-10 dataset.

4.3 Benchmarking the ResNet50 Classifier on corrupted images

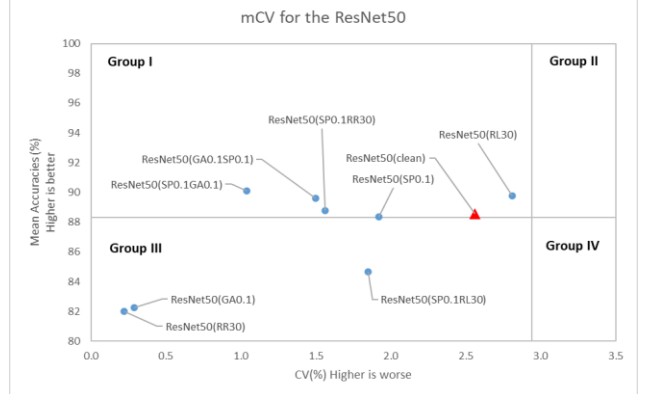


Figure 5. The mCV plot for the ResNet50 DL classifier after corrupted image sets were used to train it on the CIFAR-10 dataset. The red triangle represents $\text{Accu}(\text{ResNet50}_{\text{clean}}^{\text{alltests}})$, and blue points represent training on different corrupted image sets, i.e., examples of $\text{Accu}(\text{ResNet50}_{\text{corrupt}}^{\text{alltests}})$.

In Figure 5, the red triangle shows the ResNet50 classifier trained on clean data. The blue points are from the ResNet50 classifiers trained on different corrupted image sets. From Figure 5, we see that:

1. The training datasets affected prediction CVs of the ResNet50 classifiers. After training ResNet50 classifiers on corrupted images, the highest CVs (with the exception of CVs (with the exception of $\text{Accu}(\text{Resnet50}_{\text{RL30}}^{\text{alltests}})$)) are less than for the DL classifier trained on clean images.
2. Training ResNet50 on corrupted images can partially improve the mean accuracy during testing. $\text{Accu}(\text{Resnet50}_{\text{RL30}}^{\text{alltests}})$, $\text{Accu}(\text{Resnet50}_{\text{GA0.1SP0.1}}^{\text{alltests}})$, and

$\text{Accu}(\text{Resnet50}_{\text{SP0.1RL30}}^{\text{alltests}})$, and $\text{Accu}(\text{Resnet50}_{\text{SP0.1GA0.1}}^{\text{alltests}})$ are greater than $\text{Accu}(\text{Resnet50}_{\text{clean}}^{\text{alltests}})$.

4.4 Benchmarking the VGG-19 Classifier on corrupted images

As shown in Figure 6, the red triangle represents the VGG19 classifier trained on clean data. The green points are for the ResNet50 classifiers trained on corrupted image sets. From Figure 6, we learn that comparing $\text{CV}(\text{VGG19}_{\text{corrupt}}^{\text{alltests}})$ and $\text{CV}(\text{VGG19}_{\text{clean}}^{\text{alltests}})$, $\text{CV}(\text{VGG19}_{\text{clean}}^{\text{alltests}})$ is greater than any $\text{CV}(\text{VGG19}_{\text{corrupt}}^{\text{alltests}})$.

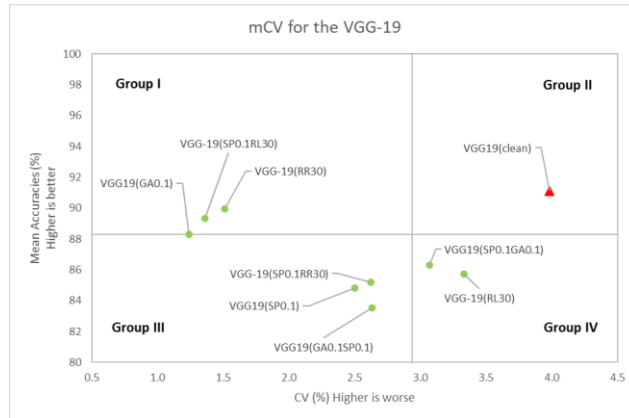


Figure 6. The mCV plot for VGG19 after corrupted image groups trained the DL classifier on the CIFAR-10 dataset. The red triangle is $\text{Accu}(\text{VGG19}_{\text{clean}}^{\text{alltests}})$, and green points are $\text{Accu}(\text{VGG19}_{\text{corrupt}}^{\text{alltests}})$.

5 DISCUSSIONS

Our tests demonstrate that high accuracy of DL classifiers on high quality image sets does not ensure high stability of DL classifiers when used on images of lowered quality such as are common in real world applications. From the merged performance data of three DL classifiers in Table 1, we conclude that:

1. Most $\text{CV}(\mathbf{D}_{\text{corrupt}}^{\text{alltests}})$ values are less than the corresponding $\text{CV}(\mathbf{D}_{\text{clean}}^{\text{alltests}})$ values. In other words, corrupted images tend to improve the robustness of DL classifiers.
2. In different DL classifiers, the same training corrupted image sets may reduce or improve the accuracies of DL classifiers. For the VGG19 classifier, the $\text{Accu}(\text{VGG19}_{\text{SP0.1RR30}}^{\text{alltests}})$ value is less than $\text{Accu}(\text{VGG19}_{\text{clean}}^{\text{alltests}})$, which means that training on corrupted image groups reduced the accuracy of VGG19. However, the ResNet50 and AlexNet classifiers show different results. For example, $\text{Accu}(\text{Alexnet}_{\text{SP0.1RR30}}^{\text{alltests}})$ is greater than $\text{Accu}(\text{Alexnet}_{\text{clean}}^{\text{alltests}})$.
3. When training sets could be either the clean image set or a corrupted image set, $\text{Accu}(\mathbf{D}_{\text{clean}}^{\text{alltests}})$ is greater than $\text{Accu}(\mathbf{D}_{\text{corrupt}}^{\text{alltests}})$ for at least most types of corruption within training sets.

Table 1. Comparing accuracy of DL classifiers on training using clean data vs. corrupted data. Training on original, uncorrupted data is denoted as "(clean)"; "(SP0.1GA01)" indicates training on an image set corrupted first by salt-and-

pepper noise at a level of 0.1 followed by Gaussian corruption at the 0.1 level. Testing is on the 69 test sets.

DL Classifier (training set)	CV (%)	Mean Accuracy (%)	Accuracy (clean) (%)
AlexNet (clean)	2.28	85.25	92.08
AlexNet (SP0.1GA0.1)	0.37	82.17	91.30
AlexNet (GA0.1)	1.04	89.67	90.90
AlexNet (GA0.1SP0.1)	2.08	89.77	90.82
AlexNet (SP0.1)	1.83	91.18	90.78
AlexNet (RR30)	1.33	89.75	90.74
AlexNet (RL30)	0.12	81.97	90.72
AlexNet (SP0.1RR30)	2.08	89.77	90.52
AlexNet (SP0.1RL30)	1.33	89.44	89.96
ResNet50 (clean)	2.56	88.56	91.18
ResNet50(SP0.1RL30)	1.85	84.66	84.16
ResNet50(RL30)	2.81	89.78	83.80
ResNet50(RR30)	0.22	81.99	83.68
ResNet50(GA0.1SP0.1)	1.50	89.60	82.56
ResNet50(SP0.1)	1.92	88.36	82.40
ResNet50(GA0.1)	0.29	82.27	82.40
ResNet50(SP0.1RR30)	1.56	88.79	82.34
ResNet50(SP0.1GA0.1)	1.04	90.08	81.90
VGG19 (clean)	3.98	91.13	94.92
VGG19(GA0.1SP0.1)	2.63	83.54	92.82
VGG19(GA0.1)	1.24	88.30	92.48
VGG19(SP0.1GA0.1)	3.07	86.33	92.16
VGG19(SP0.1)	2.50	84.83	92.16
VGG-19(SP0.1RL30)	1.36	89.34	90.48
VGG-19(RL30)	3.33	85.75	90.32
VGG-19(RR30)	1.51	89.94	90.04
VGG-19(SP0.1RR30)	2.62	85.20	88.72

To measure the correlation coefficient between CV, mean accuracy, and accuracy (clean), Spearman's rank correlation coefficient and Pearson correlation coefficient were used, as shown in Table 2.

Table 2. Spearman's Rank & Pearson Correlation Coefficient. The first column is data sets. "CV: mean Accuracy" denotes that the data sets of CV and the data sets of mean Accuracy.

Data Sets	Spearman's Rank	Pearson Correlation Coefficient
CV: mean Accuracy	0.202	0.096
CV:Accuracy(clean)	0.345	0.365
Mean Accuracy: Accuracy(clean)	0.057	0.052

From Table 2, the values of correlation coefficients are all less than 0.37. Note also that the values of correlation coefficient between CV, mean accuracy, and accuracy(clean) are not significant. In other words, these three variables are at least somewhat independent.

A robust DL classifier [16][13] should produce results with high accuracies and small CVs. While accuracy and CV are, individually, one-dimensional metrics, we integrated them into a two-dimensional metric by designing and using the mCV plot for understanding DL classifier robustness. Thus we show how to use the mean accuracy and CV together to visualize robust DL classifiers on a statistical plot. Another advantage of the mCV plot is that it provides a visualization tool for measuring robust DL classifiers with a low learning curve. This complements the standard tools used in related work like tables, line diagrams, and bar charts. This is the first study that focuses on using two-factor corruptions on images for benchmarking DL classifiers, an objective supported by the mCV plot graphic.

Third, we created 69 benchmarking image sets, including a clean set, sets with single factor corruptions, and sets with two-factor corruption conditions. The datasets and source codes are publicly available as a resource for future investigations.

Finally, previous researchers have indicated that corrupted image sets reduce the accuracy of classifiers [12] or trigger underfit [16]. We have found that this appears to be a result of using only high quality image sets for training/testing. Our results indicate that it is advantageous to include corrupted image sets during training. However, our results were partially consistent with [16] and [12]. When testing on clean images, our results were consistent with previous researchers' reports. Nevertheless, when choosing 69 testing image sets, our results confirmed that DL classifiers can enhance their robustness by training these classifiers on defective images degraded by two-factor corruptions.

There may be some potential limitations in this research. The first is the datasets. the CIFAR-10 image sets are small datasets that do not present all images. Also, the CIFAR-10 data does not have any grayscale pictures. The second limitation concerns the 68 corrupted image sets that were degraded by SP corruptions, GA corruptions, and rotations. However, these corrupted image sets do not constitute all types of imperfections that may distort images.

6 CONCLUSION

In this research, we provided a two-dimensional metric that integrates accuracy and coefficient of variation and, to display it, the mCV plot. This approach is useful for benchmarking robustness of DL classifiers. We recommended a view of robustness based on training and testing using image sets that have been deliberately corrupted to model the imperfections of images inherent in many real world application problems. Based on the foregoing, our studies serve as a proof-of-concept that mean accuracies and CVs can be used for quantitatively benchmarking robustness in the performance of DL classifiers.

In this study, we tested three DL classifiers on images degraded by two-factor corruptions. The research demonstrated that the two-factor corruption images can increase the dependability of DL classifiers and, more generally, that imperfect images should certainly be considered in training, testing and benchmarking DL classifiers.

ACKNOWLEDGMENT

The authors are grateful to Google for awarding \$5000 in cloud credits for this research in 2019.

REFERENCES

- [1] "Standard Performance Evaluation Corporation," SPEC. [Online]. Available: <http://www.spec.org/>.
- [2] "Transaction Processing Performance Evaluation Corporation," TPC. [Online]. Available: [http://www\(tpc.org/](http://www(tpc.org/).
- [3] "Storage Performance Corporation," SPC. [Online]. Available: <http://www.spcresults.org/>.
- [4] W. Dai and D. Berleant, "Benchmarking Contemporary Deep Learning Hardware and Frameworks: A Survey of Qualitative Metrics," *2019 IEEE First Int. Conf. Cogn. Mach. Intell.*, pp. 148–155, Dec. 2019, doi: 10.1109/CogMI48466.2019.00029.
- [5] D. Gershgorin, "The Data That Transformed AI Research—and Possibly the World," *Quartz, July*, vol. 26, 2017.
- [6] R. Geirhos, D. H. J. Janssen, H. H. Schütt, J. Rauber, M. Bethge, and F. A. Wichmann, "Comparing deep neural networks against humans: object recognition when the signal gets weaker," *arXiv Prepr. arXiv1706.06969*, 2017.
- [7] S. Dodge and L. Karam, "A study and comparison of human and deep learning recognition performance under visual distortions," in *2017 26th International Conference on Computer Communications and Networks, ICCCN 2017*, 2017, doi: 10.1109/ICCCN.2017.8038465.
- [8] N. Carlini and D. Wagner, "Adversarial examples are not easily detected: Bypassing ten detection methods," in *Proceedings of the 10th ACM Workshop on Artificial Intelligence and Security*, 2017, pp. 3–14.
- [9] A. Kurakin, I. Goodfellow, and S. Bengio, "Adversarial machine learning at scale," *arXiv Prepr. arXiv1611.01236*, 2016.
- [10] A. Madry, A. Makelov, L. Schmidt, D. Tsipras, and A. Vladu, "Towards deep learning models resistant to

[11] adversarial attacks," *arXiv Prepr. arXiv1706.06083*, 2017.

[12] H. Hosseini, B. Xiao, and R. Poovendran, "Google's cloud vision API is not robust to noise," in *Proceedings - 16th IEEE International Conference on Machine Learning and Applications, ICMLA 2017*, 2018, doi: 10.1109/ICMLA.2017.0-172.

[13] S. Dodge and L. Karam, "Understanding how image quality affects deep neural networks," in *2016 eighth international conference on quality of multimedia experience (QoMEX)*, 2016, pp. 1-6.

[14] D. Hendrycks and T. G. Dietterich, "Benchmarking Neural Network Robustness to Common Corruptions and Surface Variations," *arXiv Prepr. arXiv1807.01697*, 2018.

[15] S. Dodge and L. Karam, "Quality resilient deep neural networks," *arXiv Prepr. arXiv1703.08119*, 2017.

[16] W. Dai, "Benchmarking Deep Learning Robustness on Images with Two-Factor Corruption." ProQuest Dissertations Publishing, Little Rock, Arkansas, 2020.

[17] S. Zheng, Y. Song, T. Leung, and I. Goodfellow, "Improving the robustness of deep neural networks via stability training," in *Proceedings of the IEEE Computer Society Conference on Computer Vision and Pattern Recognition*, 2016, doi: 10.1109/CVPR.2016.485.

[18] Y. Cohen and J. Y. Cohen, *Statistics and Data with R: An applied approach through examples*. 2008.

[19] G. F. Reed, F. Lynn, and B. D. Meade, "Use of coefficient of variation in assessing variability of quantitative assays," *Clin. Diagn. Lab. Immunol.*, 2002, doi: 10.1128/CDLI.9.6.1235-1239.2002.

[20] T. R. FRANCIS and L. W. KANNENBERG, "YIELD STABILITY STUDIES IN SHORT-SEASON MAIZE. I. A DESCRIPTIVE METHOD FOR GROUPING GENOTYPES," *Can. J. Plant Sci.*, 1978, doi: 10.4141/cjps78-157.

Table 3. Corruption types. Type 1 or "CLEAN" represents clean images group or original images group, whereas Type 8 or "(SP0.1GA0.2)" indicates training on an image set corrupted first by salt-and-pepper noise at a level of 0.1 followed by Gaussian corruption at the 0.2 level.

1	2	3	4	5	6	7	8	9
CLEAN	SP0GA0.1	SP0GA0.15	SP0GA0.2	SP0.1GA0	SP0.1GA0.1	SP0.1GA0.1	SP0.1GA0.2	SP0.15GA0
10	11	12	13	14	15	16	17	18
SP0.15GA0.1	SP0.15GA0.1	SP0.15GA0.2	SP0.2GA0	SP0.2GA0.1	SP0.2GA0.1	SP0.2GA0.2	GA0SP0.1	GA0SP0.15
19	20	21	22	23	24	25	26	27
GA0SP0.2	GA0.15SP0	GA0.15SP0.1	GA0.15SP0.1	GA0.15SP0.2	GA0.1SP0	GA0.1SP0.1	GA0.1SP0.1	GA0.1SP0.2
28	29	30	31	32	33	34	35	36
GA0.2SP0	GA0.2SP0.1	GA0.2SP0.1	GA0.2SP0.2	SP0RR30	SP0RR60	SP0.1RR30	SP0.1RR60	SP0.15RR30
37	38	39	40	41	42	43	44	45
SP0.15RR60	SP0.2RR30	SP0.2RR60	SP0RL30	SP0RL60	SP0.1RO0	SP0.1RL30	SP0.1RL60	SP0.15RO0
46	47	48	49	50	51	52	53	54
SP0.15RL30	SP0.15RL60	SP0.2RO0	SP0.2RL30	SP0.2RL60	RR30SP0.1	RR30SP0.15	RR30SP0.2	RR30SP0
55	56	57	58	59	60	61	62	63
RR60SP0.1	RR60SP0.15	RR60SP0.2	RR60SP0	RO0SP0.1	RO0SP0.15	RO0SP0.2	RL30SP0	RL30SP0.1
64	65	66	67	68	69			
RL30SP0.15	RL30SP0.2	RL60SP0	RL60SP0.1	RL60SP0.15	RL60SP0.2			